Open beauty production

Felix Sefkow

Physik-Institut der Universität Zürich
Winterthurerstr. 190, CH-8057 Zürich, Switzerland

E-mail: felix.sefkow@desy.de

Abstract. We review measurements of open beauty production at HERA, with emphasis on recent results based on lifetime signatures. The beauty cross sections in photoproduction and deep-inelastic scattering are found to be higher than expected in QCD at next-to-leading order. The discussion includes new results on beauty production in e^+e^-, $\gamma\gamma$ and $\bar{p}p$ interactions. An outlook on the potential for measurements with the upgraded HERA collider and experiments is also given.

1. Introduction

Almost 25 years after the discovery of the b quark in proton nucleus collisions [1], the accurate understanding of how b quarks are being produced in hadronic environments is still an open issue. The subject of beauty production has recently received renewed interest, with the advent of new measurements at the ep collider HERA, and elsewhere.

The dominant mechanism for the production of heavy quarks at HERA is photon gluon fusion: a photon coupling to the scattered electron interacts with a gluon from the proton by forming a quark antiquark pair, e.g. $b\bar{b}$. A quantitative description of the process requires the knowledge of the gluon momentum distribution in the proton, the calculation of the hard photon gluon subprocess, and a fragmentation function which accounts for the long-range effects binding the heavy quark in a hadron. The gluon density in the relevant range of momentum fraction x and at the appropriate scales is known to an accuracy of a few percent from the analysis of scaling violations of the proton structure function F_2 measured at HERA [2]. The partonic process has been calculated in QCD, at next-to-leading order (NLO). The masses of the charm, and even more so of the beauty quark ensure that at least one hard scale is present that renders QCD perturbation theory to be applicable. The fragmentation function is extracted from e^+e^- annihilation data, where the kinematics of the hard process is well determined by a clean initial state. New results on b fragmentation, with significantly improved precision, have appeared recently [3, 4] and are included in this review. With such precise ingredients, b production at HERA provides a QCD testing ground *par excellence*. The validity range of the perturbative methods and the universality of non-perturbative phenomenological inputs can be closely examined.

Understanding heavy quark production is furthermore essential for the proton structure analysis of inclusive deep-inelastic scattering (DIS) data [2] in terms of parton distribution functions, since final states with charm account for about a quarter of the inclusive rate in the kinematic domain probed at HERA [5]. As shown in more detail in [6], the QCD picture sketched above has proven very successful in describing the experimental results on charm production in DIS [5, 7]. The limit of small photon virtuality is equivalent to charm photoproduction. Even in this regime, the picture works reasonably well [7, 8, 9], albeit some further clarification is needed with regard to the treatment of resolved photon processes, where the photon flutuates into a hadronic state which interacts with the proton. Evidently, it is of particular interest to subject the theory to an independent test with beauty production data.

The NLO QCD calculations of heavy quark production follow two basic approaches; for a more profound discussion see [10]. The cross section for e.g. photoproduction of heavy hadrons factorizes and can be expressed as convolutions of parton distribution functions for photon and proton, $f_i^{\gamma,p}(x_{\gamma,p})$, respectively, the partonic cross section $\hat{\sigma}_{i,j}$ (i, j denoting the parton type), and a non-perturbative fragmentation function $D(z)$, which maps the subsequent transition of the produced heavy quark into an observable heavy hadron, retaining a fraction z of the heavy quark's momentum, symbolically

$$\sigma_{\gamma p} = \sum_{i,j} f_i^{\gamma}(x_\gamma) \otimes f_j^{p}(x_p) \otimes \hat{\sigma}_{i,j} \otimes D(z) \; . \tag{1}$$

In the so-called massive scheme, only light quarks and gluons are active partons in the initial state. The heavy quark mass m_Q sets the scale for the perturbative expansion of $\hat{\sigma}$ which has been evaluated up to $\mathcal{O}(\alpha_s^2)$, including mass effects. If a second and different large scale is present, e.g. at large transverse momentum of the heavy quarks, $p_T \gg m_Q$, these calculations acquire large logarithms of the ratio p_T/m_Q, and the fixed order result becomes less reliable. In "resummed" calculations [11, 12], in the so-called massless approach, the leading terms of this type are absorbed in scale-dependent fragmentation functions, which obey the Altarelli-Parisi evolution equations. Different schemes exist for the construction of fragmentation functions. The heavy quarks are treated in the same way as the light quarks. They appear in the initial state structure functions for proton and photon and contribute via flavour excitation processes to the production of heavy quark final states. However, mass effects in the partonic cross section are neglected. The massive and the massless approach thus have complementary ranges of applicability – low and high p_T – which do not necessarily overlap. Recently, "merged" calculations interpolating between the schemes have appeared [13]. Only in the massless scheme, the factorization theorem guarantees the universality of the fragmentation functions extracted from e^+e^- data. For the scale-independent function $D(z)$ in the massive scheme, this remains an assumption based on less rigorous arguments.

The HERA results for beauty are so far limited by small statistics and dominated by production near threshold. The calculations supposed to be appropriate in this regime follow the fixed order 'massive' approach and are available in the form of Monte Carlo integration programs for photoproduction [14] and DIS [15]. Due to the higher quark

mass, the QCD predictions are expected to be more reliable for beauty than for charm. However, we note that the NLO corrections to the predicted HERA cross section are around 40% of the LO result in both cases.

In the next section the measurements performed at HERA will be presented in detail and confronted with theoretical expectations. In a subsequent section, results from other production environments will be summarized. e^+e^- data on fragmentation and measurements of beauty production cross sections in $\bar{p}p$ and $\gamma\gamma$ collisions will be presented and compared with QCD calculations which follow the same principles as for ep collisions. In the last part, we will come back to HERA and discuss the potential offered by the HERA upgrade programme [16, 17] for further studies in the field.

2. Measurements of beauty production at HERA

Beauty production at HERA is suppressed by two orders of magnitude with respect to charm, due to the larger mass and smaller electric charge of the b quark. The total cross section is dominated by photoproduction. Final states are characterized by a steeply falling p_T spectrum, which represents a challenge for secondary vertex detection. With $m_b/m_c \sim 3$, the minimally required momentum fractions of the initial state gluon is about 10 times higher than for charm production; typical values of x are around 10^{-2} and extend up to a few times 10^{-1}. The corresponding boosts relative to the laboratory frame are such that most b quarks produced at HERA are emitted under central rapidities into detector regions well covered by existing [18] or to be commissioned [17] Silicon tracking devices.

All HERA measurements of b production so far rely on inclusive semi-leptonic decays, using identified muons or electrons in dijet events. A beauty candidate with a distinctive two-jet structure and the clean signature of a penetrating muon track is shown in figure 1. In order to discriminate the b signal from background sources, two

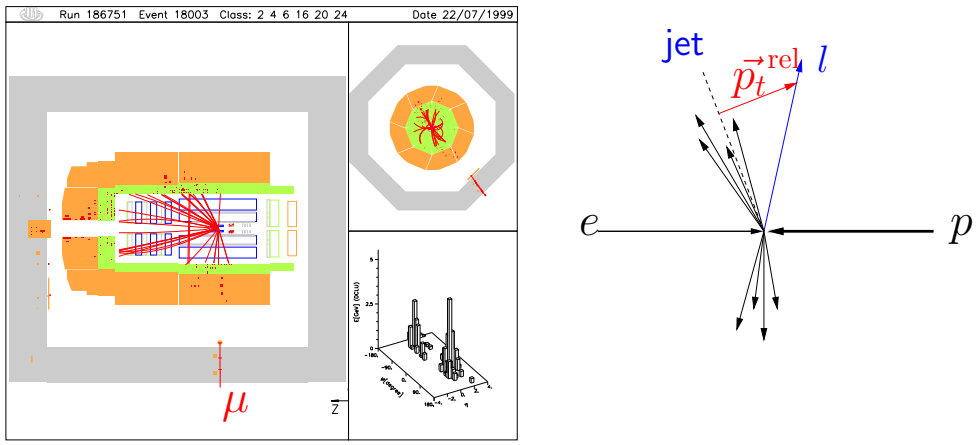

Figure 1. A beauty candidate in the H1 detector; definition of p_T^{rel}.

observables have been used which are based on the mass of the b quark or on its lifetime.

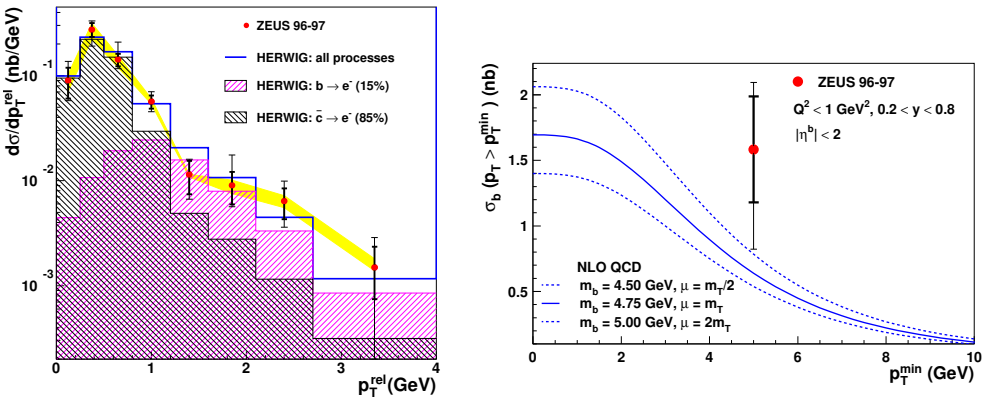

Figure 2. Cross section for the production of electrons in dijet events, as a function of p_T^{rel}; extrapolated b quark cross section compared with NLO QCD.

The high mass gives rise to large values of the transverse momentum p_T^{rel} of the decay lepton relative to the direction of an associated jet (see figure 1). Both collaborations have published photoproduction results [19, 20] using this method. More recently, with the precision offered by the H1 vertex detector [18] it has become possible to observe tracks from secondary b vertices and to exploit the long lifetime as a b tag.

The ZEUS analysis has been discussed in its preliminary version at the previous Ringberg workshop [21] and has meanwhile been published [20]. It uses electrons which are identified in the ZEUS detector by means of the topology of calorimetric energy deposition and of the specific energy loss dE/dx measured in the central track detector. Background from hadrons misidentified as electrons is statistically subtracted. Non-prompt electrons, mostly from photon conversions, are identified on the basis of track topology and invariant mass criteria. From a sample of e^+p data corresponding to an integrated luminosity of 38.5 pb^{-1}, a signal of 943 ± 69 electrons attributed to heavy quark decays is extracted. Performing the procedure in bins of p_T^{rel} and correcting for efficiency, the differential cross section shown in figure 2 is obtained. Overlaid is the result of a Monte Carlo simulation of beauty and charm production, using the HERWIG generator [22]. The normalization is adjusted to that of the data, and the shape is fitted by varying the relative contributions of charm and beauty. The fit yields a beauty fraction of $f_b = (14.7 \pm 3.8)\,\%$ in the sample, close to the HERWIG expectation of 16 %. This is translated into a cross section for the visible kinematic range,

$$\sigma^{b\to e^-}_{e^+p\to e^+ + \mathrm{dijet} + e^- + X} = 24.9 \pm 6.4^{+4.2}_{-7.3}\ \mathrm{pb} \qquad (2)$$

The range is defined by the requirements on the photon virtuality, $Q^2 < 1$ GeV^2, the inelasticity variable $0.2 < y < 0.8$, the jet rapidity $|\eta| < 2.4$, the transverse jet energy $E_T^{\mathrm{jet}} > 7(6)$ GeV for the (second) most energetic jet, the transverse momentum $p_T^{\mathrm{e}} > 1.6$ GeV and rapidity $|\eta| < 1.1$ of the electron.

In a similar manner, the cross section has also been measured as a function of x_γ, an observable which is calculated from the energies and rapidities of the jets and which in the leading-order picture corresponds to the momentum fraction of the parton in

the resolved photon entering the hard process. (For direct interactions of the photon $x_\gamma \approx 1$.) The x_γ spectrum allows a resolved contribution of $(28 \pm 5(stat.))$ % to be estimated in this picture. The HERWIG expectation is 35 %, which in this program is mostly due to flavour excitation in the photon. Due to the small beauty component in the sample, this does not allow conclusions on the b production dynamics to be drawn, but it corroborates earlier observations on charm, made by ZEUS with D^* mesons in dijet events [9].

The visible cross section can directly be compared with leading order Monte Carlo predictions, which are 8 pb for HERWIG [22] and 18 pb for PYTHIA [23] (also including flavour excitation). The recently developed CASCADE program [24], based on unintegrated parton distributions and the CCFM evolution equation [25], follows a different approach to account for higher order QCD effects. As shown in a separate contribution to this workshop [26], the approach is able to reproduce results on b production at the Tevatron. The CASCADE prediction for HERA in the ZEUS kinematic range is 18 pb [27].

In order to compare the measured cross sections with QCD predictions, the Monte Carlo simulation is used to convert the result into a b quark cross section for a range restricted in terms of parton kinematic variables to $p_T^{\mathrm{b}} > 5$ GeV, $|\eta^{\mathrm{b}}| < 2$ and to the same Q^2 and y range as above. The result,

$$\sigma^{\mathrm{ext}}_{e^+p\to e^+bX} = 1.6 \pm 0.4(stat.)^{+0.3}_{-0.5}(syst.)^{+0.2}_{-0.4}(ext.)\ \mathrm{nb} \tag{3}$$

with the third error indicating the model dependence of the extrapolation, is shown in figure 2 together with the NLO QCD expectation in the massive approach, which is obtained with the FMNR program [14] and drawn as a function of the minimal p_T^{b} requirement. The theoretical curve lies below the measurement.

The first observation of b production at HERA by H1 [19] was based on the p_T^{rel} method, too, and has also been presented at the previous workshop of this series [21]. We focus here on the more recent work based on the lifetime signature, which improves the photoproduction result [28] and provides a first measurement in DIS [29].

The H1 central silicon tracker (CST) [18] consists of two cylindrical layers of silicon strip detectors, surrounding the beam pipe at radii of $R = 57.5$ mm and $R = 97$ mm, respectively, from the beam axis. With an effective length of 358 mm it covers a large part of the ep interaction region and has a polar angle acceptance of $30^0 < \theta < 150^0$ for the outer layer, for particles emanating from the nominal interaction point. Double sided silicon detectors with readout strip pitches of 50 μm and 88 μm provide resolutions of 12 μm in $r\phi$ and 25 μm in z. The analyses presented here are performed in the transverse plane. For tracks with CST hits in both layers, the achieved resolution of the transverse distance dca to the center of the H1 detector can be parameterized as $\sigma_{dca} \approx 40\ \mu\mathrm{m} \oplus 100\ \mu\mathrm{m}/p_T[\mathrm{GeV}]$. The first term represents the intrinsic resolution and the second the contribution from multiple scattering in the beam pipe.

A magnified view of the vertex region of the event of figure 1 is displayed in figure 3. The tracks measured in the CST are represented as bands with widths corresponding

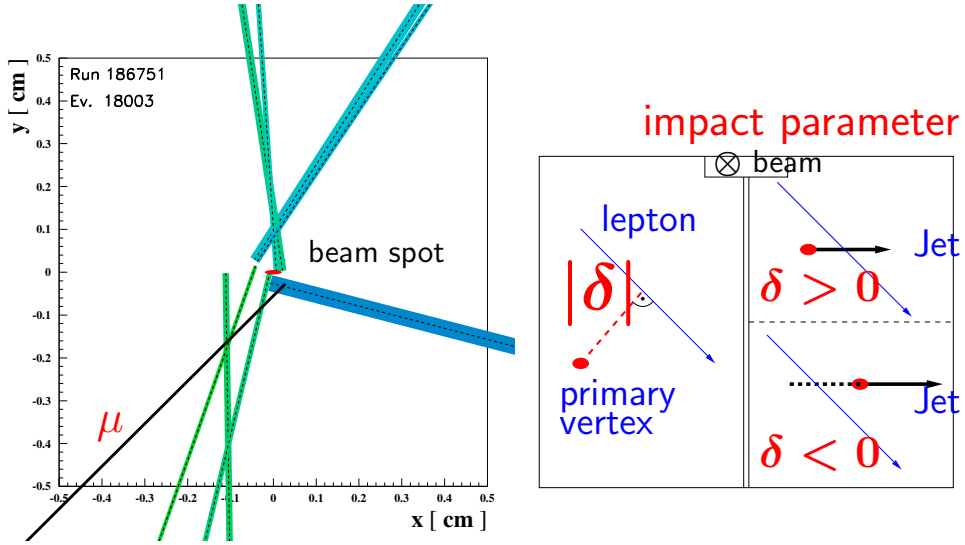

Figure 3. Vertex region of the event in figure 1 (view transverse to the beam); definition of the impact parameter δ.

to their $\pm 1\sigma$ precision. The resolution provided by the CST reveals that the muon track originates from a secondary vertex well separated from the beam spot ellipse. A simple and robust technique to exploit such signatures is using the impact parameter δ. Its magnitude is given by the *dca* of the track to the primary event vertex, and its sign is positive or negative, depending on the intercept of the track with the jet axis being downstream or upstream of the primary vertex (see figure 3). Decays of long-lived particles are signalled by positive impact parameters, whereas the finite track resolution yields a symmetric distribution.

In order to establish the method, the lifetime-based analysis is performed by applying a similar selection of dijet events with identified muons as for the published p_T^{rel} analysis in photoproduction. Jets are reconstructed here using the inclusive k_t algorithm [30] and required to have transverse energies $E_T > 5$ GeV. For each muon candidate track, the impact parameter δ is calculated, which requires the precise knowledge of the ep interaction point. The transverse profile of the interaction region at HERA has a Gaussian width of about 150 μm in the horizontal and of about 40 μm in the vertical direction. Average beam coordinates determined from many consecutive events are used to constrain the primary vertex fit applied to CST measured tracks in each individual event, excluding the muon track under consideration. A typical δ resolution of 90 μm has been achieved with comparable contributions from the muon track and from the primary vertex.

DIS and photoproduction events are analyzed separately according to whether or not the beam positron is scattered into the main detector. Shown in figure 4 is the impact parameter distribution for the photoproduction data which correspond to an integrated luminosity of $\mathcal{L} = 14.7$ pb^{-1} and contain 1403 events with $N_\mu = 1415$ muon candidates. The spectrum is decomposed by a maximum likelihood fit which adjusts the relative

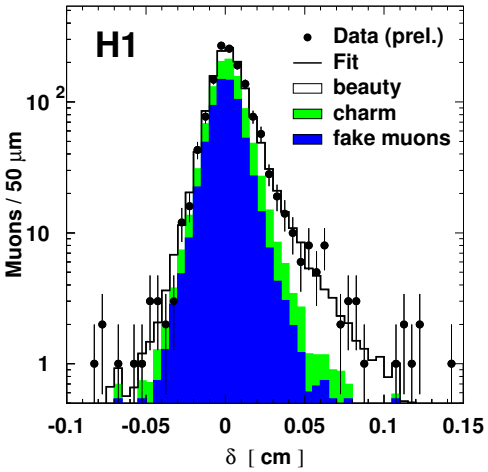

Figure 4. Muon impact parameter distribution for the photoproduction sample and decomposition from the likelihood fit.

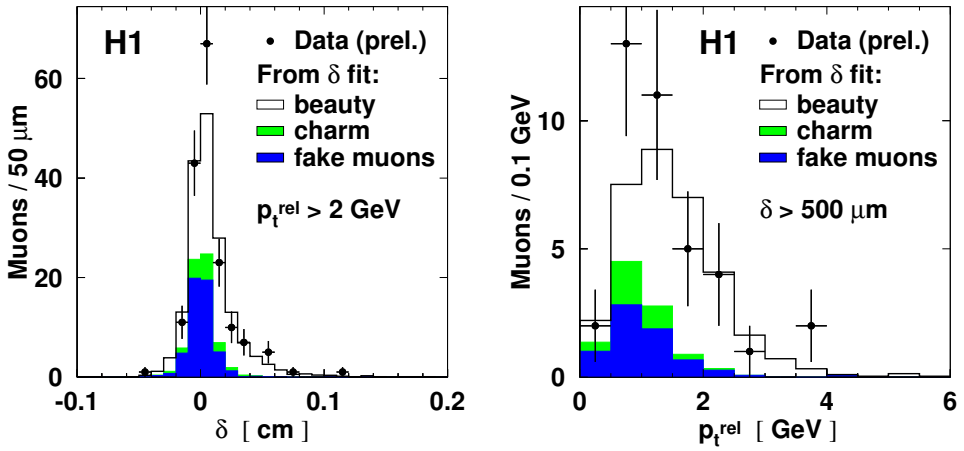

Figure 5. Muon impact parameter and p_T^{rel} distributions for b enriched photoproduction samples, with estimated contributions.

contributions from beauty, charm and fake muons to the sample. The fit describes the data well and yields a b fraction of $26 \pm 5\,\%$, which translates into a visible cross section of $\sigma^{vis}_{ep\to b\bar{b}X\to\mu X} = 159 \pm 30 \pm 29$ pb in the kinematic range defined by $p_T(\mu) > 2$ GeV, $35^\circ < \theta(\mu) < 130^\circ$ and $Q^2 < 1$ GeV^2, $0.1 < y < 0.8$. Using an independent signature and new data, this confirms the published result, $\sigma^{vis}_{ep} = 176 \pm 16\ ^{+27}_{-17}$ pb in the same range [19]. The fitted charm fraction is also compatible with the H1 measurement of D^* photoproduction [8].

To further establish the consistency of the sample composition in the two observables δ and p_T^{rel}, the b component in the events is enriched by restricting the range of one variable and then studying the distribution of the other. Figure 5 shows the observed δ spectrum after a p_T^{rel} cut. The different contributions shown in Figure 5 are the absolute predictions for the limited p_T^{rel} region, evaluated from the δ fit to the full sample. The observed impact parameter spectrum and the fit prediction, with a

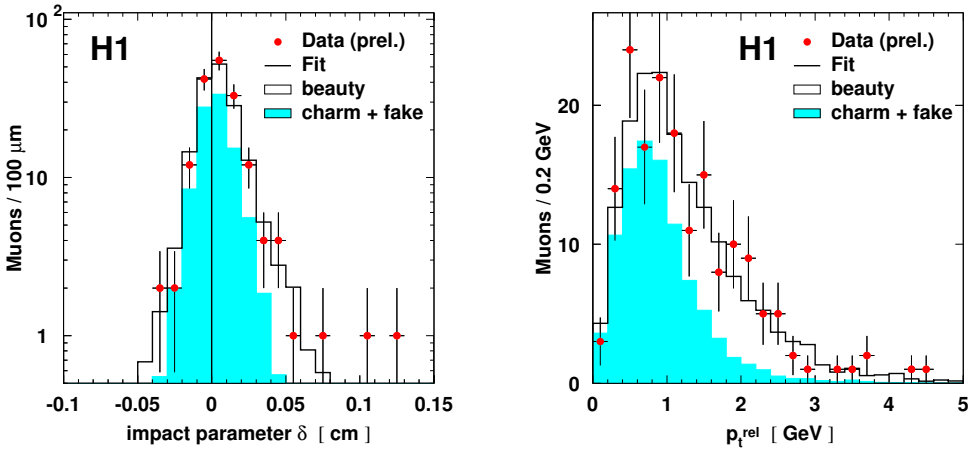

Figure 6. Muon impact parameter and p_T^{rel} distributions for DIS, with decomposition from the likelihood fit.

dominating beauty component, agree within errors. *Vice versa*, the p_T^{rel} spectrum after a cut on δ agrees within errors with the fit prediction for a b enriched sample. Since the two observables are consistent and only weakly correlated, they can be combined in a likelihood fit to the two-dimensional (δ, p_T^{rel}) distribution. It yields $f_b = (27 \pm 3)\,\%$ and

$$\sigma^{vis}_{ep\to b\bar{b}X\to\mu X} = 160 \ \pm \ 16 \pm 29 \text{ pb}, \tag{4}$$

which is again consistent with the previous H1 result [19]. The average, taking correlated systematic uncertainties into account, is $\sigma^{vis}_{ep} = 170 \pm 25$ pb .

The analysis of the smaller DIS sample relies on the sensitivity of the combined likelihood fit to the two-dimensional distribution in δ and p_T^{rel}. Using the same jet and muon requirements as in the photoproduction case, 171 candidates are selected from a dataset corresponding to 10.5 pb^{-1}. The projections of the (δ, p_T^{rel}) distribution are shown in figure 6 together with the decomposition from the fit which yields a $b\bar{b}$ fraction of $f_b = (43 \pm 8)\,\%$. Both variables are well described. The need for a sizable $b\bar{b}$ component is evident from the lifetime based signature as well as from the p_T^{rel} spectrum. The fit does not allow to disentangle the background sources themselves with meaningful accuracy, but the b fraction is only weakly sensitive to the relative amount of charm and fake muons in the background. The DIS cross section in the kinematic range given by $2 < Q^2 < 100$ GeV^2, $0.05 < y < 0.7$, $p_T(\mu) > 2$ GeV and $35^\circ < \theta(\mu) < 130^\circ$ is

$$\sigma^{vis}_{ep\to b\bar{b}X\to\mu X} = \ 39 \ \pm \ 8 \ (stat.) \ \pm 10 \ (syst.) \ \text{ pb} \ . \tag{5}$$

The visible cross sections can be directly compared to NLO QCD calculations using the FMNR [14] and HVQDIS [15] programs which provide the option to scale the b quark momenta with a Peterson fragmentation function [31] in order to obtain b hadron momenta. The distributions were folded with a lepton spectrum for b decays extracted from the AROMA [32] Monte Carlo generator. The results are 54 ± 9 pb for photoproduction and 11 ± 2 pb for DIS, where the error is predominantly due to the b quark mass uncertainty. The expectations are much lower than the H1 measurements.

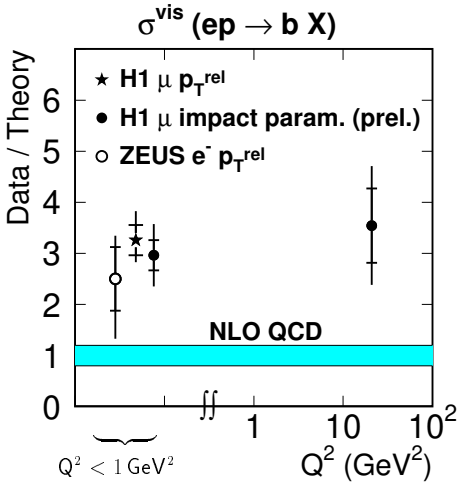

Figure 7. Ratio of measured b production cross sections at HERA over theoretical expectation, as a function of Q^2.

The data have also been compared with the LO Monte Carlo predictions. The AROMA program [32], following a "massive" approach, gives 38 and 9 pb for photoproduction and DIS, respectively. The CASCADE Monte Carlo results [24, 27] of 66 pb and 15 pb, respectively, also fall considerably below the measurements.

We note that both the H1 and ZEUS experiments observe only a tiny fraction of the total phase space. In photoproduction, the seen numbers of events correspond to 25 pb (H1) and 4 pb (ZEUS). This difference is partially due to different jet energy and y ranges and to the fact that ZEUS uses only e^-, but H1 muons of both signs and in addition includes a contribution of about 15% of secondary muons. Both experiments extrapolate by comparable factors‡ to compare with theory, but in different ways. ZEUS corrects for the lepton selection and translates the jet cuts into quark kinematics, whereas H1 keeps the lepton cuts but corrects for the jet requirements altogether. The measurements can best be compared when normalized to the same theory. However, the comparisons of the experimental results with calculations and with each other are still affected by the uncertainties related to the extrapolations. That these uncertainties are sufficiently assessed by using the various available models, remains an assumption not yet backed by experimental data. To reduce them, the distributions and correlations characterizing the final state topologies must be constrained by more refined measurements.

We summarize the HERA results as a function of Q^2 in Fig. 7. Displayed is the ratio of the measured cross sections over theoretical expectations based on the NLO QCD calculations [14, 15]. The ratio is consistent with being independent of Q^2; which indicates that the discrepancy between data and theory is not a feature of the photoproduction regime alone. At larger Q^2, resolved contributions involving the partonic structure of the photon are expected to be suppressed [33], the DIS case is

‡ Note that the ZEUS cross section is corrected for the semileptonic branching ratio, while the H1 cross section is not.

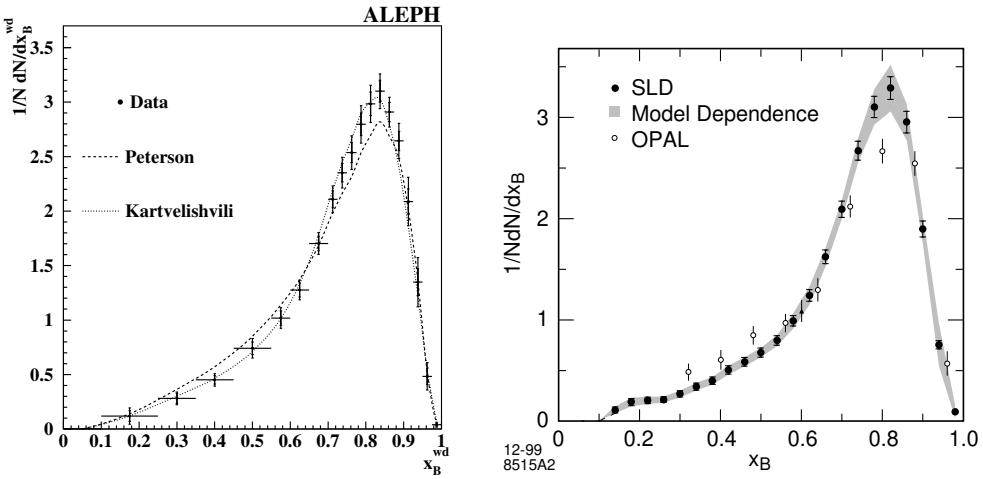

Figure 8. Measurements of the b hadron fragmentation function.

therefore complementary and theoretically cleaner.

3. Beauty production in e^+e^-, $\gamma\gamma$ and $\bar{p}p$ interactions

The theoretical understanding of b production data must always revert to a description of the fragmentation process, since only hadrons can be observed experimentally. Since the formation of hadrons involves non-perturbative effects of long-range binding forces, it cannot be calculated from first principles. Yet, e^+e^- collisions provide a clean laboratory to study the process directly and to extract the non-perturbative parameters of the fragmentation function. This is nowadays best done using data taken at the Z resonance, where millions of $e^+e^- \rightarrow Z \rightarrow b\bar{b}$ events have been recorded. One observes the distribution of $x_B = E_{wd}/E_{beam}$, the fractional energy of the weakly decaying b hadron, normalized to the maximally available energy. Final data from LEP and SLC with unprecedented precision are now becoming available. Figure 8 shows results published by ALEPH [3], using $D^{(*)}$ meson lepton correlations, and by SLD [4], using an inclusive secondary vertexing technique. Earlier OPAL results [34] with larger errors are shown for comparison; preliminary data from SLD, with even higher statistical precision, have also been released [35]. The ALEPH data are compared to two Monte Carlo simulations, which are using different functional forms [31, 36] for the parameterization of the non-perturbative fragmentation function. The Peterson form does not describe the data well; a similar observation is made by SLD [4].

Several comments are in order here. The observed x_B spectra reflect the effects of perturbative gluon radiation and of the non-perturbative hadronization phase together; the models must include both. Conclusions from the comparison with data can only be drawn for the convolution of the two effects, which is here the combination of the Peterson function with the leading log parton shower approach [37] used to model the perturbative part in the Monte Carlo simulation. When combined with resummed NLO calculations [11, 38], the Peterson function was found to be adequate. However, the

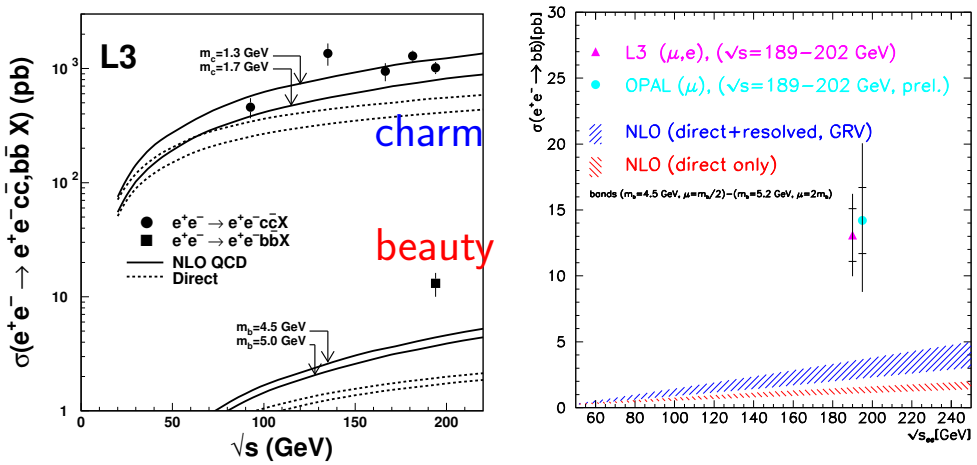

Figure 9. Measurements of charm and beauty production in two-photon collisions.

precision of the new data presents a challenge which these calculations have not yet met.

For the interpretation of the HERA measurements, these discrepancies are too small to be relevant. Altogether, the fragmentation results leave little room to modify QCD predictions for other production modes; in particular the function cannot be much harder than commonly assumed, in contrast to what would be needed to obtain larger predictions in the case of cuts on falling p_T spectra. Since the fragmentation is harder than in the charm case, the influence of the non-perturbative *versus* perturbative effects is generally suppressed. Once higher accuracy is required, one may have to turn back to the problem of how to extract a fragmentation function in a scheme consistent with the massive approach. While fixed order calculations could still provide an acceptable description of ARGUS data [39] on D^* production, this appears to be difficult in the case of B mesons produced on the Z resonance [40, 38].

With the increase of the LEP energy towards the 200 GeV range, it has become possible to observe beauty production in two-photon collisions. The process is dominated by direct and single resolved interactions, i.e. by photon-photon and photon-gluon fusion, which contribute with roughly equal strength [41]. The b quarks are predominantly produced at small p_T. They are tagged via identified electrons or muons from semileptonic decays, using the p_T^{rel} signature together with jets with as little as 3 GeV energy. The cross section, measured by L3 [42], is shown in figure 9 together with results for charm production. The NLO QCD calculations [41], shown for comparison, have been obtained in the massive approach; corrections beyond LO amount to about 30 %. While the agreement is good for charm production, the beauty cross section is underestimated by more than a factor of 2. The L3 measurement has recently been confirmed by a preliminary OPAL result [43], see figure 9.

That the pattern of results resembles the one encountered at HERA may be not accidental. There are many theoretical and experimental similarities, e.g. the necessity to model heavy quark fragmentation and jets near threshold. The QCD approach follows

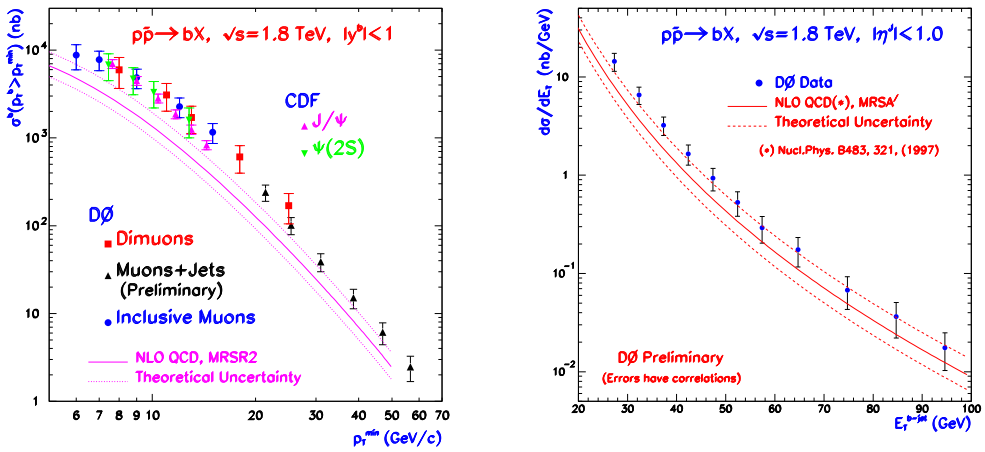

Figure 10. Measurements of the b cross section, as a function of the minimum quark p_T; b jet cross section, as a function of the jet transverse energy.

the same scheme; like in photoproduction it relies on phenomenological input to describe the hadronic structure of the photon.

The b production cross section in $\bar{p}p$ collisions has been found in excess of QCD predictions since the turn-on of the Tevatron collider [44]. At $\sqrt{s} = 1.8$ TeV gluon gluon fusion is the dominant mechanism. The measurements have meanwhile been performed using a variety of channels and techniques, and they cover a large range in transverse momentum. Results from CDF and D0 are summarized in figure 10. The two experiments are consistent with each other. There are still new results being released, for example using signals of exclusively reconstructed B^+ mesons [45], which by virtue of secondary vertex detection reside on low background and allow measurements with very small systematic uncertainty. In general, the cross section is found to be above the NLO QCD expectation [46]. However, the figure shows that the excess cannot be absorbed in a simple scaling factor, but has some p_T dependence. We also note that an increase of the excess with rapidity is observed [47]. While these results are based on b hadron detection, it has been suggested to measure the b tagged jet cross section instead [48]. The theoretical calculation should be safer against soft and collinear effects, and the confrontation with data less sensitive to assumptions on the fragmentation process. The preliminary jet data from D0 [49] are also shown in figure 10. Indeed, the agreement with theory is better. Yet, there is a similar trend for the data to be higher than the central prediction, so that no disagreement between the two sets of results can be claimed.

The longstanding discrepancy between b hadroproduction data and theory has stimulated speculations about possible explanations beyond the standard model. For example, a scenario [50] in the context of minimal supersymmetry, with relatively light gluinos $\tilde{g}$ and sbottom quarks $\tilde{b}$, can easily reproduce the data, as demonstrated in figure 11. There are further consequences that can be tested at the Tevatron; for HERA however, first estimates indicate only small effects in this particular scenario. It is nevertheless interesting to note that such an interpretation is not ruled out by existing experimental constraints, including the e^+e^- continuum data and precision

measurements or direct searches performed at the Z and $\Upsilon(4S)$ resonances (see [50] and references therein).

A more conventional approach is to refine the QCD calculations. The large scale dependence, which is still present at NLO, indicates that important contributions are missing in the perturbative expansion of the cross section. In figure 11, the B meson cross section [51] is compared to a resummed calculation [52] in the massless scheme, using perturbative fragmentation functions directly adjusted to LEP data. A good description is found, surprisingly also for the data at lower p_T, where the agreement for this scheme is considered as fortuitous by the authors of [52]. However, a similar "surprise" was found in the case of charm photoproduction at HERA [7, 9]. A cross section enhancement in the medium p_T range of the Tevatron data is also found, using high p_T resummation via fragmentation functions in a different scheme [53]. There are other resummation strategies being pursued [24, 54], namely using the concept of unintegrated parton densities, which is discussed in more detail in [26]. These approaches lead to enhancements of the predictions.

The experimental precision can be expected to improve even further, when results from the upgraded Tevatron become available, and this should provide additional guidelines to find out which strategy most effectively includes the missing higher oder contributions. In either case, whether speculations on supersymmetry will further be nourished, or whether "only" the QCD techniques will be refined, complementary information from HERA will be extremely valuable. Apart from e^+e^- annihilation, DIS represents the cleanest b production environment.

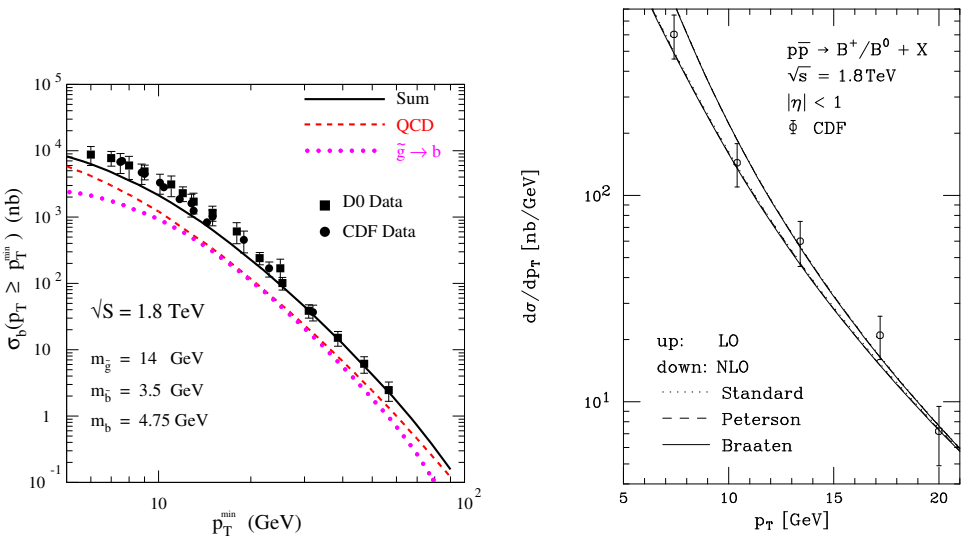

Figure 11. b cross section data, compared with a model assuming light supersymmetric sbottom quark production; CDF data in comparison with a resummed NLO QCD calculation in the massless scheme.

4. Prospects for the HERA upgrade

The HERA collider is currently resuming its operation, after an upgrade which lays the foundations for an integrated luminosity of 1 fb^{-1} to be accumulated in the next 5 years. Much of the experimental upgrade program which was pursued in parallel by the H1 [16] and ZEUS [17] collaborations is directed towards augmenting the capabilities for heavy quark physics, notably by improving the acceptance and precision of the tracking systems, in particular for forward-going particles, and by enhancing the trigger sensitivity for final states with small p_T.

The HERA results on beauty production are statistically limited, and it is evident that higher luminosity would be beneficial. Here we ask more specifically the question whether it will be possible to vary the two scales p_T^2 and Q^2 independently and over a range extending significantly beyond the one set by the quark mass, $4m_b^2$. This would open kinematic regions to investigate the regime most relevant for improving the perturbative QCD calculation. Figure 12 shows the estimated number of beauty candidates to be expected if the H1 muon analysis described in section 2 would be extended in its present form to the full anticipated HERA II statistics. The event yield is displayed as a function of the transverse momentum of the b quark in the hadronic centre-of-mass system. Reasonable results can be obtained with samples of about 100 events.

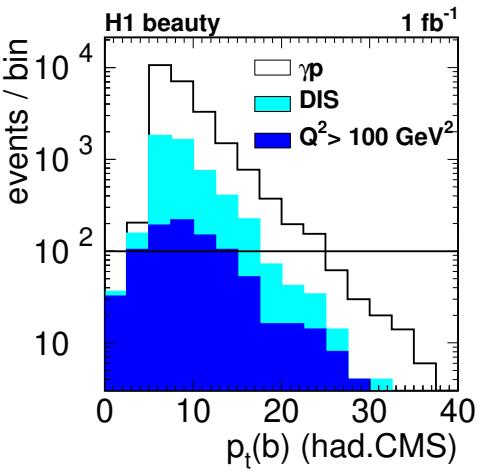

Figure 12. Estimated numbers of events, as a function of the b quark transverse momentum in the partonic CMS, for an extension of the present H1 muon analysis to the expected full HERA data set.

Thus, in photoproduction (DIS) measurements up to $p_T \approx 25(15)$ GeV will be possible. In the high Q^2 regime, more inclusive techniques will be needed to extend the range beyond $p_T \approx 10$ GeV. With the correlation of x and Q^2 at HERA in mind, one can foresee meaningful tests of low x or high p_T resummation approaches.

ZEUS is presently being equipped with a micro-vertex detector [17], while first results obtained with the H1 silicon tracker have been described here. A major goal is to apply inclusive secondary vertex tagging methods with algorithms similar to those used

at the Tevatron or at LEP, where they provided very pure b samples with efficiencies of 20 % and higher. Impact parameter resolutions at HERA are similar, and the luminosity upgrade by means of stronger beam focusing has the appreciated side effect of reducing the size of the interaction region to 80×20 μm^2, to be compared with 110×10 μm^2, e.g. at LEP. It is difficult to seriously predict b tagging efficiencies for HERA, because they depend crucially on how effectively charm and light quark background can be suppressed; excellent control of tracking systematics is a key issue here. The method will work the better, the higher p_T and thus the vertexing accuracy is. It can complement the more exclusive channels in the region where they suffer most from limited statistics. It will be interesting to check at HERA whether the better description of b jet data found in $\bar{p}p$ interactions (figure 10) is a general feature.

Extending the measurements, on the other hand, towards low p_T holds the promise of reducing the model uncertainties related to the extrapolations into the region where the cross section is largest. This could be achieved by replacing the semi-leptonic signature relying on jets by (semi-)exclusive decay modes involving reconstructed D^* or J/Ψ mesons. Due to the higher background levels at lower p_T, enhanced discrimination power is required online to fully benefit from the higher luminosity. H1 is installing new systems [16] using latest generation electronics, which will allow to detect invariant mass signatures at the trigger level. ZEUS plans to incorporate the vertex detector into the trigger.

Finally, both experiments are upgrading their forward tracking systems with new drift chambers and silicon detectors [17, 16]. This will increase the lever arm in x (and Q^2) for QCD studies, probe the gluon distribution in a different region, up to $x \gtrsim 0.1$, and give better access to the region where resolved photon processes are important. Moreover, since at HERA the production of heavy particles, due to necessarily large x values involved, leads to final states boosted into the forward direction, these upgrades will open possibilities to use beautiful signatures in searches for new physics, for example the anomalous production of single top quarks, for which candidates exist [55], but not with a b tag.

In conclusion, in disclosing beauty at HERA, we are entering a field which is experimentally challenging, theoretically rewarding, and potentially exciting.

Acknowledgments

It is a pleasure to thank the organizers for composing a stimulating meeting, as unique and irreplaceable as its venue. I am indebted to E. Elsen, L. Gladilin, B. Kniehl and M. Kuze for their careful reading of the manuscript.

References

[1] S. W. Herb *et al.*, Phys. Rev. Lett. **39** (1977) 252.

[2] C. Adloff *et al.* [H1 Collaboration], Eur. Phys. J. C **21** (2001) 33 [hep-ex/0012053]; J. Breitweg *et al.* [ZEUS Collaboration], Eur. Phys. J. C **7** (1999) 609 [hep-ex/9809005].

[3] A. Heister *et al.* [ALEPH Collaboration], Phys. Lett. B **512** (2001) 30 [hep-ex/0106051].
[4] K. Abe *et al.* [SLD Collaboration], Phys. Rev. Lett. **84** (2000) 4300 [hep-ex/9912058].
[5] C. Adloff *et al.* [H1 Collaboration], hep-ex/0108039; J. Breitweg *et al.* [ZEUS Collaboration], Eur. Phys. J. C **12** (2000) 35 [hep-ex/9908012].
[6] I. Redondo, these proceedings.
[7] C. Adloff *et al.* [H1 Collaboration], Nucl. Phys. B **545** (1999) 21 [hep-ex/9812023].
[8] S. Aid *et al.* [H1 Collaboration], Nucl. Phys. B **472** (1996) 32 [hep-ex/9604005].
[9] J. Breitweg *et al.* [ZEUS Collaboration], Eur. Phys. J. C **6** (1999) 67 [hep-ex/9807008]; Phys. Lett. B **481** (2000) 213 [hep-ex/0003018].
[10] G. Kramer, *In *Tegernsee 1999, New trends in HERA physics* 275-289.*
[11] B. A. Kniehl, M. Kramer, G. Kramer and M. Spira, Phys. Lett. B **356** (1995) 539 [hep-ph/9505410]; B. A. Kniehl, G. Kramer and M. Spira, Z. Phys. C **76** (1997) 689 [hep-ph/9610267]; J. Binnewies, B. A. Kniehl and G. Kramer, Z. Phys. C **76** (1997) 677 [hep-ph/9702408]; Phys. Rev. D **58** (1998) 014014 [hep-ph/9712482].
[12] M. Cacciari and M. Greco, Phys. Rev. D **55** (1997) 7134 [hep-ph/9702389].
[13] M. Cacciari, S. Frixione and P. Nason, JHEP **0103** (2001) 006 [hep-ph/0102134]; S. Frixione, M. Cacciari and P. Nason, hep-ph/0107063.
[14] S. Frixione, M. L. Mangano, P. Nason and G. Ridolfi, Nucl. Phys. B **412** (1994) 225 [hep-ph/9306337]; Phys. Lett. B **348** (1995) 633 [hep-ph/9412348].
[15] B. W. Harris and J. Smith, Phys. Rev. D **57** (1998) 2806 [hep-ph/9706334].
[16] H1 Collaboration, proposals DESY PRC 98/02; 98/06; 99/01; 99/02; 99/06; A. Baird *et al.* [H1 Collaboration], Nucl. Instrum. Meth. A **461** (2001) 461; S. Luders *et al.*, hep-ex/0107064.
[17] A. Garfagnini, Nucl. Instrum. Meth. A **435** (1999) 34; B. Foster, hep-ex/0107066.
[18] D. Pitzl *et al.*, Nucl. Instrum. Meth. A **454** (2000) 334 [hep-ex/0002044].
[19] C. Adloff *et al.* [H1 Collaboration], Phys. Lett. B **467** (1999) 156 [hep-ex/9909029], and Erratum (to be published).
[20] J. Breitweg *et al.* [ZEUS Collaboration], Eur. Phys. J. C **18** (2001) 625 [hep-ex/0011081].
[21] D. Pitzl, *In *Tegernsee 1999, New trends in HERA physics* 265-274.*
[22] G. Marchesini, B. R. Webber, G. Abbiendi, I. G. Knowles, M. H. Seymour and L. Stanco, Comput. Phys. Commun. **67** (1992) 465.
[23] H. Bengtsson and T. Sjostrand, Comput. Phys. Commun. **46** (1987) 43.
[24] H. Jung and G. P. Salam, Eur. Phys. J. C **19** (2001) 351 [hep-ph/0012143].
[25] M. Ciafaloni, Nucl. Phys. B **296** (1988) 49; S. Catani, F. Fiorani and G. Marchesini, Nucl. Phys. B **336** (1990) 18; Phys. Lett. B **234** (1990) 339.
[26] H. Jung, these proceedings.
[27] H. Jung, private communication.
[28] F. Sefkow, hep-ex/0011034.
[29] T. Sloan, hep-ex/0105064.
[30] S. Catani, Y. L. Dokshitzer, M. H. Seymour and B. R. Webber, Nucl. Phys. B **406** (1993) 187.
[31] C. Peterson, D. Schlatter, I. Schmitt and P. Zerwas, Phys. Rev. D **27** (1983) 105.
[32] G. Ingelman, J. Rathsman and G. A. Schuler, Comput. Phys. Commun. **101** (1997) 135 [hep-ph/9605285].
[33] M. Gluck, E. Reya and M. Stratmann, Phys. Rev. D **54** (1996) 5515 [hep-ph/9605297].
[34] G. Alexander *et al.* [OPAL Collaboration], Phys. Lett. B **364** (1995) 93.
[35] K. Abe *et al.* [SLD Collaboration], SLAC-PUB-8504 *Contributed to 30th International Conference on High-Energy Physics (ICHEP 2000), Osaka, Japan, 27 Jul - 2 Aug 2000.*
[36] V. G. Kartvelishvili, A. K. Likhoded and V. A. Petrov, Phys. Lett. B **78** (1978) 615.
[37] T. Sjostrand, Comput. Phys. Commun. **82** (1994) 74.
[38] P. Nason and C. Oleari, Nucl. Phys. B **565** (2000) 245 [hep-ph/9903541].
[39] H. Albrecht *et al.* [ARGUS Collaboration], Z. Phys. C **52** (1991) 353.
[40] P. Nason and C. Oleari, Phys. Lett. B **447** (1999) 327 [hep-ph/9811206].

[41] M. Drees, M. Kramer, J. Zunft and P. M. Zerwas, Phys. Lett. B **306** (1993) 371.
[42] M. Acciarri *et al.* [L3 Collaboration], Phys. Lett. B **503** (2001) 10 [hep-ex/0011070].
[43] A. Csilling [OPAL Collaboration], hep-ex/0010060.
[44] F. Abe *et al.* [CDF Collaboration], Phys. Rev. Lett. **71** (1993) 500; Phys. Rev. Lett. **71** (1993) 2396; Phys. Rev. D **53** (1996) 1051 [hep-ex/9508017]; Phys. Rev. D **55** (1997) 2546; S. Abachi *et al.* [D0 Collaboration], Phys. Rev. Lett. **74** (1995) 3548; Phys. Lett. B **370** (1996) 239; B. Abbott *et al.* [D0 Collaboration], Phys. Lett. B **487** (2000) 264 [hep-ex/9905024];
[45] V. Papadimitriou [CDF Collaboration], FERMILAB-CONF-00-234-E.
[46] P. Nason, S. Dawson and R. K. Ellis, Nucl. Phys. B **303** (1988) 607; Nucl. Phys. B **327** (1989) 49 [Erratum-ibid. B **335** (1989) 260].
[47] B. Abbott *et al.* [D0 Collaboration], Phys. Rev. Lett. **84** (2000) 5478 [hep-ex/9907029].
[48] S. Frixione and M. L. Mangano, Nucl. Phys. B **483** (1997) 321 [hep-ph/9605270].
[49] B. Abbott *et al.* [D0 Collaboration], Phys. Rev. Lett. **85** (2000) 5068 [hep-ex/0008021].
[50] E. L. Berger, B. W. Harris, D. E. Kaplan, Z. Sullivan, T. M. Tait and C. E. Wagner, Phys. Rev. Lett. **86** (2001) 4231 [hep-ph/0012001].
[51] A. Laasanen [CDF Collaboration], FERMILAB-CONF-96-198-E.
[52] J. Binnewies, B. A. Kniehl and G. Kramer, Phys. Rev. D **58** (1998) 034016 [hep-ph/9802231].
[53] M. Cacciari, M. Greco and P. Nason, JHEP **9805** (1998) 007 [hep-ph/9803400].
[54] P. Hagler, R. Kirschner, A. Schafer, L. Szymanowski and O. Teryaev, Phys. Rev. D **62** (2000) 071502 [hep-ph/0002077]; R. D. Ball and R. K. Ellis, JHEP **0105** (2001) 053 [hep-ph/0101199].
[55] C.Vallee [H1 Collaboration], presented at EPS 2001, July 2001